ELSEVIER

Journal of Molecular Structure 604 (2002) 87–99

Journal of
MOLECULAR
STRUCTURE

www.elsevier.com/locate/molstruc

Rotamerisation and intramolecular proton transfer of 2-(2′-hydroxyphenyl)oxazole, 2-(2′-hydroxyphenyl)imidazole and 2-(2′-hydroxyphenyl)thiazole: a theoretical study

Pradipta Purkayastha[a], Nitin Chattopadhyay[a,b,*]

[a]*Department of Chemistry, Jadavpur University, Calcutta, 700 032, India*
[b]*Department of Chemistry, Coimbra University, Coimbra, 3049, Portugal.*

Received 7 March 2001; revised 8 May 2001; accepted 8 May 2001

Abstract

Semi-empirical (AM1–SCI) calculations have been performed on 2-(2′-hydroxyphenyl)oxazole (HPO), 2-(2′-hydroxyphenyl)imidazole (HPI) and 2-(2′-hydroxyphenyl)thiazole (HPT) to rationalise the photophysical behaviour of the compounds exhibiting intramolecular rotation as well as excited state intramolecular proton transfer (ESIPT). The calculations reveal that there is a gradual variation in the properties from HPO to HPT through HPI so far as the existence of the rotational isomers in the ground state is concerned. While HPO gives rise to two stable rotamers (**I** and **II**) in all the common solvents, there is only one stable species for HPT in the S_0 state. For HPI, rotamer **II** is possible only in the isolated state and/or in solvents of low polarity, but in high polar solvents it gives rise to the normal form (**I**) only. For all the molecules in the series, however, intramolecular proton transfer (IPT) takes place in the lowest excited singlet (S_1) and the triplet (T_1) states. Combination of the rotamerism and ESIPT gives rise to multiple fluorescence bands for the fluorophores. Theoretical assignments have been made for the excitation, fluorescence and phosphorescence bands. Simulated potential energy curves (PEC) in different electronic states reveal that the IPT process is feasible in either of the S_1 and T_1 states but not in the ground state. The ESIPT reaction has been found to be favoured both thermodynamically and kinetically in these electronic states compared to the ground state. However, quantum mechanical tunnelling has been proposed for the prototropic reaction to proceed in the excited states.

Keywords: 2-(2′-Hydroxyphenyl)oxazole; 2-(2′-Hydroxyphenyl)imidazole; 2-(2′-Hydroxyphenyl)thiazole; Rotamerisation; Intramolecular proton transfer; Potential energy curve

1. Introduction

The proton transfer and/or hydrogen atom transfer from one group (—OH, —NH_2) to another (>C=O, —N=) has been recognised to be the most general and important reaction in chemistry [1]. Depending on the situation, the reaction can be intramolecular or intermolecular. The phenomenon may occur by thermal and/or photoinduced activation through a barrierless or a barrier crossing process [2]. Because of its immense potential, excited state intramolecular proton transfer (ESIPT) has generated massive interest in recent years [1–42]. This phenomenon has widespread implications in photostabilisers [3], laser dyes [4] and also in the biological fields [5]. In

* Corresponding author. Address for communication: Department of Chemistry, Jadavpur University, Calcutta-700 032, India. Tel: +91-33-483-4133; fax: +91-33-473-4266.
E-mail address: pcnitin@yahoo.com (N. Chattopadhyay).

0022-2860/02/$ - see front matter
PII: S0022-2860(01)00647-0

organic bifunctional molecules, containing both the hydrogen atom donor and acceptor groups in close proximity, an intramolecular hydrogen bond is generally formed in the ground electronic state [1]. If favoured, the hydrogen-bonded proton migrates, in the excited state, from the donor atom to the acceptor atom at a distance of <2 Å to produce a phototautomer [6]. The most striking feature of the dynamics in these systems is their ultra-fast nature and the highly Stokes-shifted fluorescence of the tautomer produced through the process [1]. It is believed that the Franck–Condon excited state of the molecule has a close proximity to the intersection with the potential energy curve (PEC) of the phototautomer and, hence, on excitation, the molecule passes to the tautomeric species almost instantaneously and then relaxes vibrationally [7–11]. The barriers to both the normal$^* \rightarrow$ tautomer* and tautomer $\rightarrow$ normal processes are very low — greater than the energies of the lowest frequency vibrations but similar to, or smaller than those of the stretching modes of the concerned compound skeleton [30]. It has thus been stated that the proton transfer comes about through the vibrational relaxation rather than thermal activation.

The azole compounds form an important class in the field of ESIPT [16–18]. There is a good number of experimental and some theoretical reports available on the photophysics of these systems in different environments [9–42]. The early studies on 2-(2′-hydroxyphenyl)benzoxazole (HBO), and 2-(2′-hydroxyphenyl)benzothiazole (HBT) were started by Cohen and Flavian [19,20] who compared the behaviours of these compounds with N-nitrosalicylideneanilines in different solvents. Woolfe et al. [21] studied the complex photophysical behaviour of HBO using steady-state absorption and fluorescence as well as picosecond time-resolved emission spectroscopy. The mechanistic aspects of ESIPT in HBO have also been studied by several workers [22–24]. The proton transfer in the excited compounds occurs from the S_1 state with very low activation energy [22]. At room temperature the decay of the photoproduced keto form is dominated by a thermally activated radiationless transition but at lower temperatures fluorescence and intersystem crossing are the main deactivation processes [23]. The effects of hydrogen tunnelling and isotopes on the keto–enol tautomerisation in HBO were added investigations [24]. Apart from different homogeneous media, HBO photophysics has also been investigated in micro-heterogeneous environments provided by the cyclodextrins [25,26]. Several theoretical works have also corroborated the experimental findings in various ways [27–29,39–42].

A solvent dependence study on the steady-state absorption, excitation and fluorescence spectra of HBI [2-(2′-hydroxyphenyl)benzimidazole] has indicated the presence of different species in the S_1 state which have the same precursor in the S_0 state [31]. ESIPT and rotamerisation of HBI have been studied using steady-state and time-resolved emission spectroscopy and also by semi-empirical quantum chemical methods [32–34]. Picosecond spectroscopic studies have been made on the ESIPT in HBT [35,36] where a change in the fluorometric behaviour of the compound in different environmental conditions has been highlighted. The temperature effect on the same phenomenon also produced interesting results [37]. Existence of different excited species for HBT in varying pH in ethanolic solution has been reported by Potter et al. [38].

Less work, comparatively, has been done on the photophysics of another similar series of compounds, namely 2-(2′-hydroxyphenyl)oxazole (HPO), 2-(2′-hydroxyphenyl)imidazole (HPI) and 2-(2′-hydroxyphenyl)thiazole (HPT) [39–41]. Douhal et al. [39] and Guallar et al. [40] have experimented with the phenyl-substituted derivatives of HPO. The former work was performed under the gas-phase isolated condition in a supersonic jet. The dispersed fluorescence of the compounds analysed, exhibited a large Stokes' shift. The results were interpreted in terms of the occurrence of a fast excited-state intramolecular proton-tunnelling-transfer reaction in the enol form, producing a keto tautomer through an asymmetric potential energy surface with a small energy barrier [39]. Guallar et al. [40] came up with both the experimental and theoretical study on HPO derivatives where they proposed that two rotamers coexist in the ground state and only one of them can undergo ESIPT.

A recent work on the 4,5-dimethyl derivative of HPI [34] throws some light on the prototropic property of the compound. Steady-state and time-resolved studies have been done in the work and

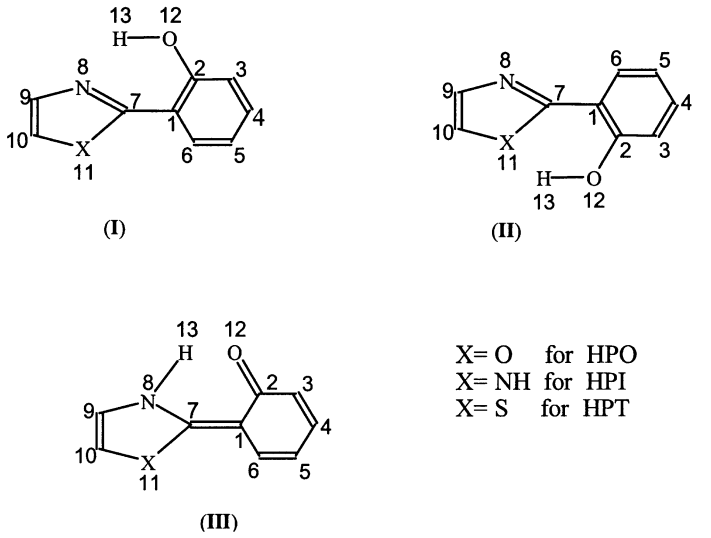

Scheme 1.

some rationalisation has been made through quantum chemical calculations. The behaviour of the HPI derivative has been reported to be very sensitive to the nature of the solvent and large differences have been observed in hydrogen-bonding solvents. In another recent work, LeGourriérec et al. have studied HPO and the 4-methyl derivative of HPT fluorometrically and noticed that the photophysical properties of the compounds highly resemble those of the corresponding benzo analogues [43]. Their quantum chemical calculations propose two deactivation channels for the photoproduced tautomer in the first excited singlet state.

In a previous work [29], we presented a theoretical investigation of the photophysical properties of HBO, HBI and HBT to understand the detail of the ground and excited state processes. We assigned the different excitation and emission bands from the semi-empirical calculations and they were found to correlate well with the experimental ones. In the present work we have extended a similar endeavour to another series of compounds, namely HPO, HPI and HPT. Apart from the studies on these compounds, the current paper also reports a survey in the comparative fields of the compounds and their benzo analogues, HBO, HBI and HBT. Although, at present, there are insufficient experimental data for the molecules of this series (particularly for HPI), for completeness of this study, we have calculated data for and assigned values to all the relevant species for all three molecular systems in the series. We believe strongly that in the near future more experimental data will become available to fill the gaps.

2. Quantum chemical calculations

Although being less explicit than the *ab initio* method, semi-empirical calculations have been established as extremely useful, particularly for large molecular systems, in explaining structures, energetics and reactivities in different electronic states. Acceptable approximations in these methods yield results close to the experimental ones [29,43–49]. The reliability of our method of calculation (AM1–SCI) has already been established through studies on different types of molecular systems varying widely in their photophysical properties [29,46–49]. The calculated molecular structural parameters have been shown to match very well with the crystallographic data for two different molecular systems, i.e. 2-(3-methoxy-2-hydroxyphenyl)benzimidazole [29] and 2-(2'-hydroxyphenyl)benzothiazole [47]. For the present work, we have used the same commercial package, HYPERCHEM 5.01 as described previously [46]. The geometry of the molecules has been optimised in the

Table 1
Equilibrium parameters of different photoisomers of HPO, HPI and HPT in different electronic states. Energy (E) and dipole moment (μ) are expressed in eV and debye units, respectively. R_{8-13} represents the interatomic distance (Å) between the two atoms referred to by the numbers (see Scheme 1). $T_{2-1-7-8}$ is the torsion angle (degrees) developed by the atoms referred to by the numbers

Molecule	Parameters	Normal (**I**)	Rotamer (**II**)	Tautomer (**III**)
HPO	E (S_0)	−93.0181	−93.0060	−92.5105
	μ (S_0)	2.08	0.87	4.58
	R_{8-13}	2.18	3.69	0.997
	$T_{2-1-7-8}$	0	150	0
	E (S_1)	−89.4435	−89.3764	−89.4581
	μ (S_1)	1.01	1.74	3.96
	$T_{2-1-7-8}$	0	170	0
	E (T_1)	−90.9033	−123.8853	−91.0296
	μ (T_1)	1.42	1.19	2.42
	$T_{2-1-7-8}$	0	180	0
HPI	E (S_0)	−96.0248	−96.0043	−95.5077
	μ (S_0)	3.88	1.97	6.33
	R_{8-13}	2.33	3.69	1.00
	$T_{2-1-7-8}$	40	140	0
	E (S_1)	−92.4601	−92.2281	−92.5831
	μ (S_1)	2.91	2.57	5.36
	$T_{2-1-7-8}$	0	140	0
	E (T_1)	−93.7735	−93.7452	−93.9393
	μ (T_1)	3.04	1.83	4.15
	$T_{2-1-7-8}$	0	180	0
HPT	E (S_0)	−92.2318	–	−91.7456
	μ (S_0)	2.54	–	4.00
	R_{8-13}	2.14	–	1.00
	$T_{2-1-7-8}$	10	–	0
	E (S_1)	−88.9889	–	−89.3397
	μ (S_1)	1.62	–	1.15
	$T_{2-1-7-8}$	0	–	0
	E (T_1)	−90.2039	–	−90.4719
	μ (T_1)	1.83	–	2.44
	$T_{2-1-7-8}$	0	–	0

ground state using the AM1 method. For the excited states, we have adopted AM1–SCI and considered all the configurations (around 130 configurations) within an energy window of 14 eV from the ground state, for the single electronic transitions only. The principle of the calculations is the same as described elsewhere [29].

The torsion angle (2–1–7–8; see Scheme 1) between the hydroxyphenyl plane and the heterocyclic plane was preset to different values and all other geometrical parameters were fully optimised to obtain the ground state energy values for each of the rotational conformers (rotamers) and hence to find their relative stability. With these optimised structures, we have performed the SCI within the stated energy window to acquire the energies and dipole moments corresponding to the ground as well as the different excited electronic states (S_0, S_1, T_1 etc.).

For the intramolecular proton transfer (IPT) reaction, we have considered the distance between the dissociable hydrogen of the hydroxyl group and the nitrogen atom (to which the hydrogen becomes attached when the tautomer is formed) involved in the process (R_{8-13}) as the reaction coordinate [29]. For the generation of the potential energy curves (PEC) for the IPT process, we have optimised the geometry with various preset values of the reaction coordinates. AM1–SCI was then applied to ascertain the energies and dipole moments of the species on the trajectory of the reaction in different electronic states. The enthalpy of reaction (ΔH) and activation energy (E_{act}) for the IPT reaction of the fluorophores

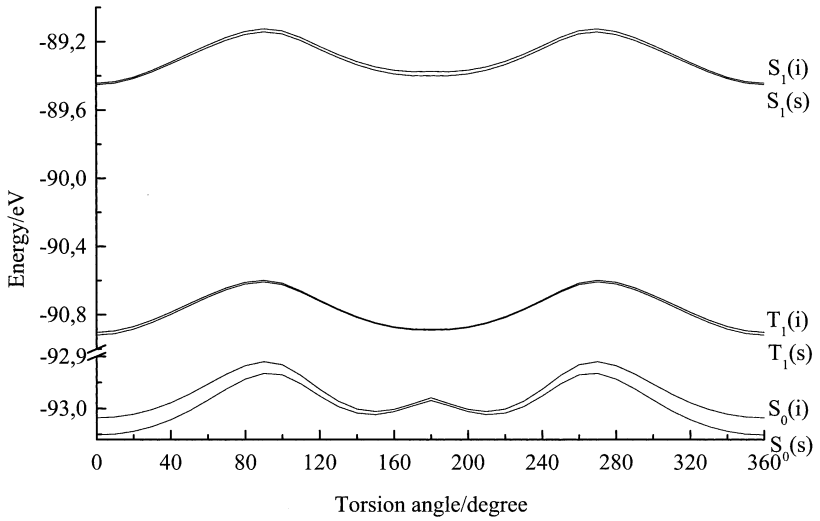

Fig. 1. Plot of total energy as a function of torsion angle (2–1–7–8) in the S_0, S_1 and T_1 states of HPO (i, isolated; s, solvated in ethanol).

have been determined from the PEC in the corresponding electronic states.

The solvent stabilisation of different states has been calculated from the solvation energy based on Onsager's continuum model [29,50]. Assuming that the solute molecule, having a dipole moment μ_i in the *i*th electronic state, to be fully solvated, the solvation energy is given by

$$\Delta E_{\text{solv.}} = \frac{2\mu_i^2(\varepsilon_r - 1)}{a^3(2\varepsilon_r + 1)}$$

where ε_r is the bulk relative permittivity of the solvent and a, the cavity radius. We have taken the maximum molecular length for the optimised geometry as the cavity diameter for the molecular systems (8.50, 8.46 and 8.72 Å for HPO, HPI and HPT, respectively). As before, specific solvent interactions like hydrogen bonding etc. have not been considered in the present work.

3. Results and discussion

As mentioned above, the applicability and reliability of our method of calculation have already been established from the comparison of the calculated and the X-ray crystallographic data for the structural parameters of two molecular systems having reaction centres very similar to the molecules of the present series, namely 2-(3-methoxy-2-hydroxyphenyl)benzimidazole [29] and 2-(2'-hydroxyphenyl)benzothiazole [47].

3.1. Intramolecular rotation

Various calculated parameters for the different rotameric and prototropic species of HPO, HPI and HPT, in different electronic states, have been tabulated in Table 1. The table clearly reflects the stability of the normal form (**I**) over the rotamer (**II**) and the tautomer (**III**) in the ground state for all three compounds.

Figs. 1–3 show the simulated energy profiles for the intramolecular rotation of the hydroxyphenyl moiety relative to the heterocyclic ring for HPO, HPI and HPT, respectively, in different electronic states to examine the existence of the different stable conformational isomers. The figures present the energy diagrams for the bare molecules along with their solvated species in ethanol.

Fig. 1 reveals the existence of both the normal (**I**) and the rotameric (**II**) forms (see Scheme 1) for HPO in the ground state. This has been corroborated from the absorption studies as well [39–43]. The calculated values of the dihedral angles for the stable normal and rotameric forms in the ground state are found to be 0° and 150°, respectively. The intrinsic steric effect due to the lone electron pair on the oxygen atom in the heterocyclic ring and its effective size is probably

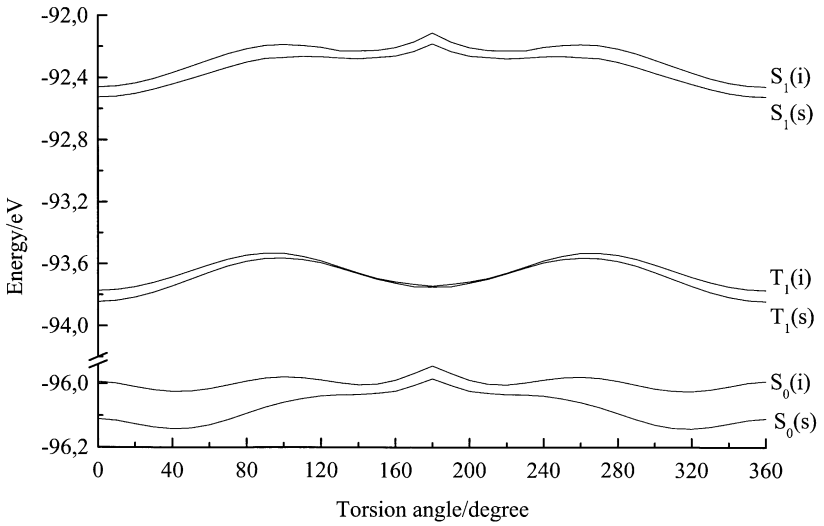

Fig. 2. Plot of total energy as a function of torsion angle (2–1–7–8) in the S_0, S_1 and T_1 states of HPI (i, isolated; s, solvated in ethanol).

responsible for the deviation of the torsional angle from 180°. Thus, HPO has a similar geometry to that of its benzo analogue, HBO, in the ground state so far as the intramolecular rotation is concerned [29]. A comparison of the difference in the energies of the S_0 and S_1 states for HPO and HBO points to a red shift of the absorption band of the latter compared to the former that has actually been observed and is ascribed to the extension of the conjugated system [43]. The rotamers (**II**) for both the compounds are less stable than the normal forms (**I**). The activation energy for the rotameric transformation **I** → **II** for HPO is about 0.108 eV in vacuum while that for HBO was calculated to be 0.101 eV. For the reverse transformation **II** → **I** the same has a magnitude of 0.105 eV and 0.096 eV for the two molecular systems, respectively.

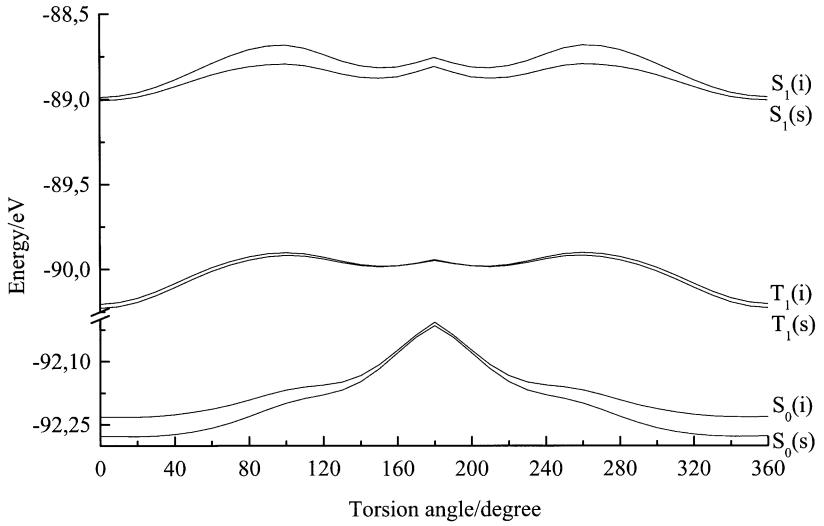

Fig. 3. Plot of total energy as a function of torsion angle (2–1–7–8) in the S_0, S_1 and T_1 states of HPT (i, isolated; s, solvated in ethanol).

Table 2
Assignment of excitation, fluorescence and phosphorescence spectra of HPO in different solvents in terms of calculated energies (eV). (n.a. indicates non-availability of data)

Solvent	Species	Excitation			Fluorescence		Phosphorescence	
		Calc.		Expt.[a]	Calc.	Expt.[a]	Calc.	Expt.[a] (ref)
		$n\pi^*$	$\pi\pi^*$					
Methylcyclohexane	**I**	3.60	3.81	3.88	3.57	n.a.	2.11	n.a.
	II	3.66	3.87	4.00	3.60	3.66	2.09	n.a.
	III	–	–	–	2.99	2.60	1.46	n.a.
p-dioxane	**I**	3.60	3.82	n.a.	3.57	n.a.	2.11	n.a.
	II	3.66	3.87	n.a.	3.60	n.a.	2.09	n.a.
	III	–	–	–	2.99	n.a.	1.46	n.a.
Ethanol	**I**	3.61	3.83	3.93	3.57	n.a.	2.10	2.30 (12)
	II	3.66	3.87	4.06	3.59	3.60	2.09	2.80 (12)
	III	–	–	–	2.93	2.70	1.44	n.a.
Acetonitrile	**I**	3.61	3.83	3.96	3.57	n.a.	2.10	n.a.
	II	3.66	3.87	4.06	3.59	3.60	2.09	n.a.
	III	–	–	–	2.93	2.70	1.43	n.a.
Water	**I**	3.61	3.83	3.98	3.57	n.a.	2.10	n.a.
	II	3.66	3.87	4.10	3.59	3.55	2.09	n.a.
	III	–	–	–	2.93	2.79	1.43	n.a.

[a] The experimental values have been taken from Ref. [43] if not otherwise mentioned.

The low energy barriers suggest that species **I** and **II** are in equilibrium at ambient temperature. Thus, HPO and HBO behave similarly so far as the existence of the rotational isomers is concerned.

Similar calculations with the HPI system yield the simulation of Fig. 2. The results reveal that in vacuo, HPI gives rise to stable normal (**I**) and the rotamer (**II**) in the ground state. Both of them coexist in solvents of low polarity like methylcyclohexane and 1,4-dioxane as well. However, in highly polar solvents, like ethanol, acetonitrile and water, the barrier for the stabilisation of the two rotational isomers hardly exists. Although a near stability zone can be achieved as shown in the figure, the distinctive stability of **I** and **II** becomes questionable in solvents of higher polarity. We do not have proper data at the moment to verify this experimentally. In the benzo analogue of HPI, i.e. HBI, however, both the normal (**I**) and the rotameric (**II**) forms coexist in all the solvents although the barrier for the inter-conversion decreases as one moves towards high polarity solvents [29]. The additional steric factor developed due to the presence of the N—H group in HPI or HBI relative to —O— in HPO or HBO probably restricts the formation of the rotamer. The activation energies for the inter-conversion of **I** → **II** in both HPI and HBI is found to be 0.045 eV in vacuo and those for the reverse process, i.e. **II** → **I** are 0.024 eV and 0.021 eV, respectively. For both HPI and HBI the normal form (**I**) and the rotamer (**II**) correspond to a dihedral angle of 40° and 140°, respectively.

Fig. 3 clearly shows that thiazole differs considerably from the other two molecules in the present series so far as rotamerisation is concerned. Neither in the isolated nor in the solvated state does it give any stabilisation to the rotamer (**II**). The recent studies of LeGourriérec et al. [42] corroborate our theoretical proposition. The authors have rationalised the non-existence of the rotamer of HPT from a greater single bond character of the bond joining the phenol and the azole rings in HPT and thus allowing for more twisting vibrations whereby the rotamer is unable to achieve any well-defined stability. HBT behaves in exactly the same way as HPT in this respect [27,29].

3.2. Assignment of the electronic spectra

In this section we have assigned the excitation, fluorescence and phosphorescence spectra of HPO, HPI and HPT in some common solvents differing in

Table 3
Assignment of excitation, fluorescence and phosphorescence spectra of HPI in different solvents in terms of calculated energies (eV). (n.a. indicates non-availability of data)

Solvent	Species	Excitation			Fluorescence		Phosphorescence	
		Calc.		Expt.	Calc.	Expt.	Calc.	Expt.
		$n\pi^*$	$\pi\pi^*$					
Methylcyclohexane	**I**	3.70	3.96	n.a.	3.51	n.a.	2.19	n.a.
	II	3.79	3.87	n.a.	3.75	n.a.	2.19	n.a.
	III	–	–	–	2.83	n.a.	1.51	n.a.
p-dioxane	**I**	3.71	3.97	n.a.	3.50	n.a.	2.19	n.a.
	II	3.79	3.87	n.a.	3.75	n.a.	2.19	n.a.
	III	–	–	–	2.82	n.a.	1.51	n.a.
Ethanol	**I**	3.77	4.03	n.a.	3.47	n.a.	2.15	n.a.
	II	–	3.88	–	–	–	–	–
	III	–	–	–	2.70	n.a.	1.43	n.a.
Acetonitrile	**I**	3.77	4.03	n.a.	3.47	n.a.	2.15	n.a.
	II	–	3.89	–	–	–	–	–
	III	–	–	–	2.70	n.a.	1.43	n.a.
Water	**I**	3.78	4.03	n.a.	3.46	n.a.	2.15	n.a.
	II	–	3.89	–	–	–	–	–
	III	–	–	–	2.69	n.a.	1.43	n.a.

polarity. Since, in pure and homogeneous solvents the solvation dynamics requires a faster time-scale than the fluorescence lifetime [51,52], the fluorophore molecule is solvated before fluorescing. Hence, the excited molecules have been considered to fluoresce from the solvated S_1 state to the corresponding Franck–Condon S_0 state. Likewise, the excitation spectra have been corroborated with the transition between the solvated S_0 and the Franck–Condon S_1 states. Similar calculations with the first excited triplet states of the molecules have been performed to give an assignment to their phosphorescence spectra. The

Table 4
Assignment of excitation, fluorescence and phosphorescence spectra of HPT in different solvents in terms of calculated energies (eV). (n.a. indicates non-availability of data)

Solvent	Species	Excitation			Fluorescence		Phosphorescence	
		Calc.		Expt.[a]	Calc.	Expt.[a]	Calc.	Expt.[a]
		$n\pi^*$	$\pi\pi^*$					
Methylcyclohexane	**I**	3.27	3.45	3.65	3.23	n.a.	2.02	n.a.
	III	–	–	–	2.40	2.37	1.26	n.a.
p-dioxane	**I**	3.27	3.45	n.a.	3.23	n.a.	2.02	n.a.
	III	–	–	–	2.40	n.a.	1.25	n.a.
Ethanol	**I**	3.30	3.47	3.72	3.22	n.a.	2.00	n.a.
	III	–	–	–	2.40	2.46	1.23	n.a.
Acetonitrile	**I**	3.30	3.47	3.72	3.22	n.a.	2.00	n.a.
	III	–	–	–	2.40	2.46	1.23	n.a.
Water	**I**	3.30	3.48	n.a.	3.22	n.a.	2.00	n.a.
	III	–	–	–	2.40	2.48	1.23	n.a.

[a] Since we do not have the experimental values for the HPT system, the data in the table refer to the spectral positions for 2-(2′-hydroxyphenyl)-4-methylthiazole and they have been taken from Ref. [43].

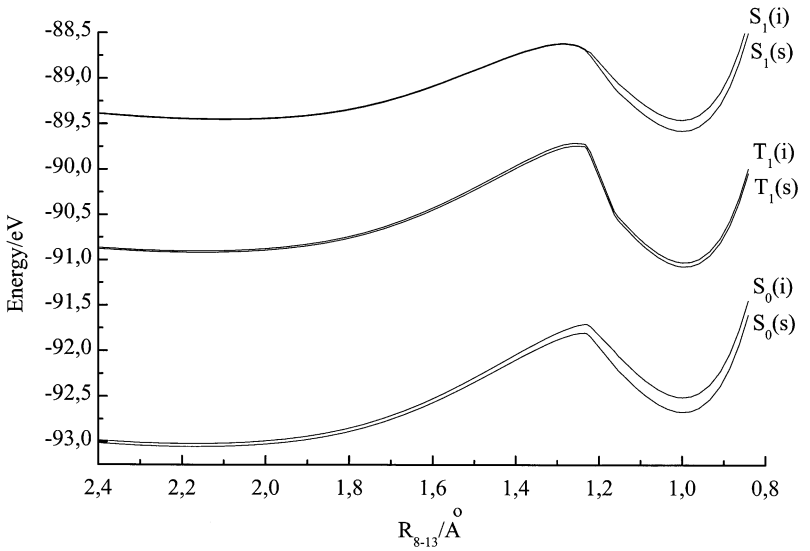

Fig. 4. Simulated potential energy curves for the IPT process of HPO in the S_0, S_1 and T_1 states (i, isolated; s, solvated in ethanol).

spectral assignments of the three molecular systems are presented in Tables 2–4. It is pertinent to mention here that the positions of the experimental absorption bands are always at a higher energy compared to the calculated absorption position. This is because the calculated spectra represent the 0–0 transition only between the S_0 and S_1 states, while the experiments give rise to absorption bands with broad maxima leading to the transition to the upper vibrational levels of S_1 as well.

It is known that for the molecular systems under study, there are two close lying excited singlet states (a lower one $n\pi^*$ and an upper one $\pi\pi^*$). The calculations show reasonably higher oscillator strengths for the excitation of the ground state species to that of the $n\pi^*$ states than to the $\pi\pi^*$ states for HPO and HPI,

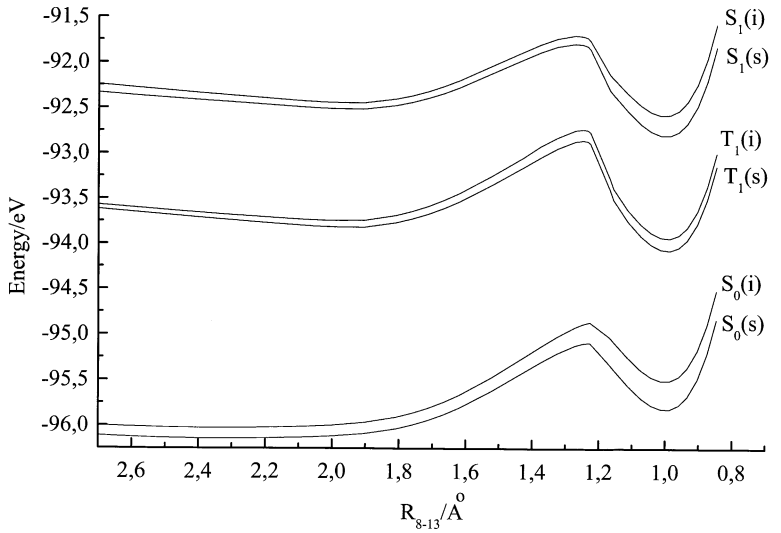

Fig. 5. Simulated potential energy curves for the IPT process of HPI in the S_0, S_1 and T_1 states (i, isolated; s, solvated in ethanol).

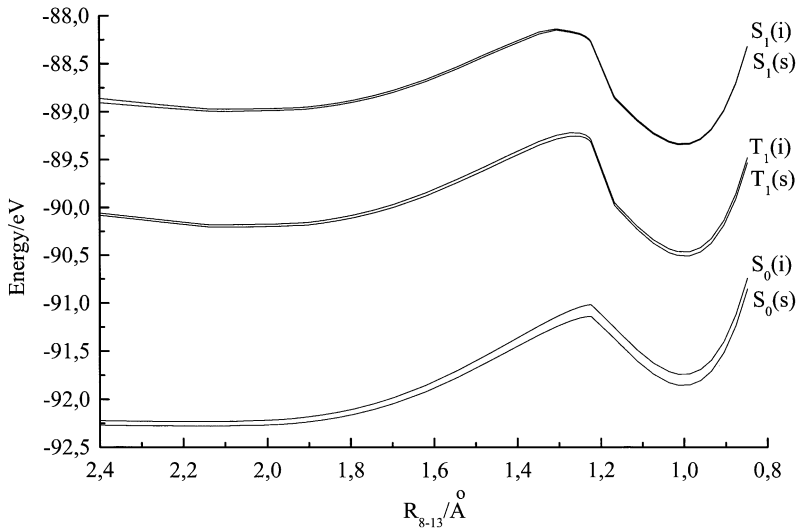

Fig. 6. Simulated potential energy curves for the IPT process of HPT in the S_0, S_1 and T_1 states (i, isolated; s, solvated in ethanol).

suggesting that the principal transition is $S_0 \rightarrow S_{n\pi^*}$. For HPT, however, the oscillator strength for the transition to the $\pi\pi^*$ state is higher than the other transition. In any case, for all the systems, the experimental absorption energy values are rather closer to the calculated S_0–$S_{\pi\pi^*}$ energy gaps (Tables 2–4 gives the transition energies from S_0 to the lowest $n\pi^*$ and $\pi\pi^*$ singlet states). It may happen that due to some specific interaction within the species themselves or with the solvents, which has not been considered in our calculations, the predominant excitation process is $S_0 \rightarrow S_{\pi\pi^*}$ rather than $S_0 \rightarrow S_{n\pi^*}$. Excitation to the higher $\pi\pi^*$ states, however, does not affect the calculated fluorescence or phosphorescence energies as the excited fluorophore equilibrates to the lowest excited singlet $n\pi^*$ state before fluorescence or phosphorescence. Thus the assignment of the fluorescence and phosphorescence bands holds.

3.3. Intramolecular proton transfer

Like the compounds of the analogous benzo series, HPO, HPI and HPT undergo excited state intramolecular proton transfer (ESIPT) only in their normal (**I**) form. The potential energy curves (PEC) for the ESIPT process have been simulated in S_0, S_1 and T_1 states considering R_{8-13} (*vide infra*) as the reaction coordinate. Figs. 4–6 represent the simulated potential energy curves for the ESIPT process of these molecular systems in the isolated state as well as in ethanol solvent.

The figures clearly reveal that for all three fluorophores, the tautomer formation [through intramolecular proton transfer (IPT)] in the ground state leads to endothermicity. However, the reaction becomes exothermic in the S_1 as well as in the T_1 state. Thus, the reaction is thermodynamically unfavourable in the ground state but it is favoured in the lowest excited singlet and triplet states. Considering the kinetic aspect, for the same reaction, our calculation reveals that the activation barrier for the process is quite high for all three systems in the ground state leading to the imposition of a restriction to the process from the kinetic point of view. This barrier is, however, reduced appreciably in the other electronic states favouring the ESIPT process in these states. Thus, it is revealed that although the IPT reaction is not allowed for these systems in the ground state, both thermodynamically as well as kinetically, the ESIPT process is favoured in the S_1 and T_1 states. Table 5 presents the values of the thermodynamic (ΔH, the reaction enthalpy) and the kinetic parameters (E_{act}, the activation energy) for HPO, HPI and HPT in different solvents. Regarding the IPT process, molecules of the present series behave similarly to the corresponding benzo analogues (Fig. 6). The magnitude of the reaction enthalpy, however, differs

Table 5
Calculated activation energies (E_{act} in eV) and reaction enthalpies (ΔH in eV) for the intramolecular proton transfer reaction of HPO, HPI and HPT in S_0, S_1 and T_1 states

Medium/Solvent	State	HPO		HPI		HPT	
		$E_{act.}$	ΔH	$E_{act.}$	ΔH	$E_{act.}$	ΔH
Vacuum	S_0	1.311	+0.508	1.159	+0.523	1.212	+0.491
	S_1	0.834	−0.010	0.744	−0.132	0.834	−0.361
	T_1	1.193	−0.126	1.009	−0.193	0.962	−0.284
Methylcyclohexane	S_0	1.283	+0.453	1.113	+0.440	1.179	+0.462
	S_1	0.835	−0.058	0.735	−0.197	0.839	−0.356
	T_1	1.186	−0.138	0.987	−0.221	0.957	−0.292
p-dioxane	S_0	1.279	+0.447	1.108	+0.431	1.175	+0.459
	S_1	0.835	−0.063	0.733	−0.204	0.840	−0.355
	T_1	1.185	−0.140	0.985	−0.224	0.956	−0.293
Ethanol	S_0	1.244	+0.380	1.051	+0.329	1.135	+0.423
	S_1	0.835	−0.122	0.722	−0.287	0.846	−0.348
	T_1	1.177	−0.155	0.957	−0.257	0.950	−0.303
Acetonitrile	S_0	1.242	+0.377	1.048	+0.324	1.133	+0.421
	S_1	0.835	−0.125	0.722	−0.287	0.846	−0.348
	T_1	1.177	−0.156	0.956	−0.259	0.950	−0.303
Water	S_0	1.241	+0.374	1.046	+0.320	1.131	+0.420
	S_1	0.835	−0.127	0.716	−0.295	0.847	−0.347
	T_1	1.177	−0.156	0.955	−0.260	0.950	−0.304

for the two series principally because of the difference in the potential energy of the normal (**I**) and the tautomer (**III**) forms owing to the presence of the additional phenyl ring fused with the heterocyclic ring in the compound of the benzo series.

It is important to note that the calculated activation barriers for the proton transfer process within the systems in their corresponding S_1 ($n\pi^*$) states are quite high (Table 5), although much lower than those in the S_0 states. Our calculated activation barriers receive support from the calculations of Guallar et al. [40] and Forés et al. [42], the first group reporting the barrier for the process in HPO in the S_1 state as 0.74 eV while the other group reporting the barrier for HPI in the lowest $n\pi^*$ singlet state as 0.67 eV. However, these barriers are too high for the proton transfer process to be manifested within the lifetime of the species in their excited S_1 states. Forés et al. have calculated a lower barrier in the $\pi\pi^*$ state of HPI. Although our calculation on HPT shows a slightly lower activation barrier (0.70 eV) in the $\pi\pi^*$ state than that in the $n\pi^*$ state, for the other two systems the calculation does not give similar results. Thus, we feel that the reaction takes place in the lowest excited $n\pi^*$ singlet states for all the molecular systems in general. Guallar et al. have considered a complex scheme for the concerted process of proton transfer and intramolecular rotation for HPO and have given an explanation for the occurrence of the proton transfer process in the excited state by considering a tunnelling mechanism [40]. Our simple model, without accommodating the concerted scheme, provides an acceptable interpretation of the feasibility of the proton transfer process in photo-excited states from the thermodynamic point of view. However, it does not provide an explanation from the kinetic side. In line with Guallar et al., we believe that the process proceeds through quantum mechanical tunnelling.

4. Conclusion

The rotamerisation and the intramolecular proton transfer in HPO, HPI and HPT construct the basis of the photophysical properties displayed by each of these molecules. We have made an effort, rather comprehensively, to sum up the behaviours of the said compounds in an isolated state and in the presence of common homogeneous solvents. The

above results and the related discussion lead to the following relevant points regarding the fluorophores:

1. In vacuum and in common solvents, HPO gives rise to two rotameric forms in the ground state through a rotation about the single bond connecting the phenol ring and the azole ring. HPT, on the other hand, offers no stability to the rotamer (**II**) leading to the existence of the normal form (**I**) only in all such conditions. For HPI, however, the rotamer (**II**) is possible only in an isolated state and/or in solvents of low polarity. In highly polar solvents it gives rise to the normal form (**I**) only.
2. All three molecular systems behave similarly as we consider the intramolecular proton transfer process. The reaction is restricted in the ground state from thermodynamic as well as kinetic considerations. Both these factors, however, favour the ESIPT process in the S_1 and T_1 states compared to the ground state. Quantum mechanical tunnelling has been proposed to be responsible for the proton transfer process to proceed.

Acknowledgements

Financial assistance from the Council of Scientific and Industrial Research and the Department of Science and Technology, Govt. of India, is gratefully acknowledged.

References

[1] E.F. Caldin, V. Gold, Proton-transfer Reactions, Chapman and Hall, London, 1975.
[2] A. Douhal, F. Lahmani, A.H. Zewail, Chem. Phys. 207 (1996) 477.
[3] D.B. O'Connor, G.W. Scott, D.R. Coulter, A. Yavroulan, J. Phys. Chem. 95 (1991) 10252.
[4] P.T. Chou, M.L. Martinez, M.A. El-Sayed, J. Phys. Chem. 97 (1993) 2618.
[5] G.C. Lin, E.S. Awad, M.A. El-Sayed, J. Phys. Chem. 95 (1991) 10442.
[6] K. Das, N. Sarkar, A.K. Ghosh, D. Majumdar, D.N. Nath, K. Bhattacharyya, J. Phys. Chem. 98 (1994) 9126.
[7] B.J. Schwartz, L.A. Peteanu, C.B. Harris, J. Phys. Chem. 96 (1992) 3591.
[8] N.P. Ernsting, Th. Arthen-Engeland, M.A. Rodriguez, W. Thiel, J. Chem. Phys. 97 (1993) 3914.
[9] W. Frey, T. Elsaesser, Chem. Phys. Lett. 189 (1992) 565.
[10] W. Wiechmann, H. Port, W. Frey, F. Lärmer, T. Elsaesser, Chem. Phys Lett. 165 (1990) 28.
[11] F. Lärmer, T. Elsaesser, W. Kaiser, Chem. Phys. Lett. 148 (1988) 119.
[12] K.C. Ingham, M.A. Elbayoumi, J. Am. Chem. Soc. 96 (1974) 1682.
[13] A. Douhal, R. Sastre, Chem. Phys. Lett. 219 (1994) 91.
[14] M. Wiechmann, H. Port, W. Frey, F. Lärmer, T. Elsaesser, J. Phys. Chem. 95 (1991) 1918.
[15] A. Douhal, J. Phys. Chem. 98 (1994) 13131.
[16] S.J. Formosinho, L.G Arnaut, J. Photochem. Photobiol. A: Chem. 75 (1993) 21.
[17] S.M. Ormson, R.G. Brown, Progr. React. Kinet. 19 (1994) 45.
[18] D. LeGourriérec, S.M. Ormson, R.G. Brown, Progr. React. Kinet. 19 (1994) 211.
[19] M.D. Cohen, S. Flavian, J. Chem. Soc. B (1967) 317.
[20] M.D. Cohen, S. Flavian, J. Chem. Soc. B (1967) 321.
[21] G.J. Woolfe, M. Melzig, S. Schneider, F. Dörr, Chem. Phys. 77 (1983) 213.
[22] A. Mordzinsky, A. Grabowska, Chem. Phys. Lett. 90 (1982) 122.
[23] A. Mordzinsky, K.H. Grellmann, J. Phys. Chem. 90 (1986) 5503.
[24] W. Al-Soufi, K.H. Grellmann, B. Nickel, J. Phys. Chem. 95 (1991) 10503.
[25] S. Kundu, S.C. Bera, N. Chattopadhyay, Ind. J. Chem. A 34 (1995) 55.
[26] E.L. Roberts, J. Dey, I.M. Warner, J. Phys. Chem. 100 (1996) 19681.
[27] S. Nagaoka, A. Itoh, K. Mukai, U. Nagashima, J. Phys. Chem. 97 (1993) 11385.
[28] S. Nagaoka, J. Kusunoki, T. Fujibuchi, K. Mukai, U. Nagashima, J. Photochem. Photobiol. A: Chem. 122 (1999) 151.
[29] P. Purkayastha, N. Chattopadhyay, Phys. Chem. Chem. Phys. 2 (2000) 203.
[30] M.A. Rios, M.C. Rios, J. Phys. Chem. 99 (1995) 12456.
[31] H.K. Sinha, S.K. Dogra, Chem. Phys. 102 (1986) 337.
[32] K. Das, N. Sarkar, D. Majumdar, K. Bhattacharyya, Chem. Phys. Lett. 198 (1992) 443.
[33] M.C.R. Rodriguez, F. Rodriguez-Prieto, M. Mosquera, Phys. Chem. Chem. Phys. 1 (1999) 253.
[34] M. Bräuer, M. Mosquera, J.L. Pérez-Lustres, F. Rodriguez-Prieto, J. Phys. Chem. 102 (1998) 10736.
[35] T. Elsaesser, B. Schmetser, Chem. Phys. Lett. 140 (1987) 293.
[36] T. Elsaesser, B. Schmetzer, M. Lipp, R.J. Bäuerle, Chem. Phys. Lett. 148 (1988) 112.
[37] C.A.S. Potter, R.G. Brown, F. Vollmer, W. Rettig, J. Chem. Soc. Faraday Trans. 90 (1994) 59.
[38] C.A.S. Potter, R.G. Brown, Chem. Phys. Lett. 153 (1988) 7.
[39] A. Douhal, F. Lahmani, A. Zehnacker-Rentien, F. Amat-Guerri, J. Phys. Chem. 98 (1994) 12198.
[40] V. Guallar, M. Moreno, J.M. Lluch, F. Amat-Guerri, A. Douhal, J. Phys. Chem. 100 (1996) 19789.
[41] L. Lavtchieva, V. Enchev, Z. Smedarchina, J. Phys. Chem. 97 (1993) 306.
[42] M. Forés, M. Duran, M. Solà, L. Adamowicz, J. Phys. Chem. A 103 (1999) 4413.

[43] D. LeGourriérec, V.A. Kharlanov, R.G. Brown, W. Rettig, J. Photochem. Photobiol. A: Chem. 130 (2000) 101.
[44] Th. Arthen-Engeland, T. Bultmann, N.P. Ernsting, M.A. Rodriguez, W. Thiel, Chem. Phys. 163 (1992) 43.
[45] B. Dick, J. Phys. Chem. 94 (1990) 5752.
[46] P. Purkayastha, P.K. Bhattacharyya, S.C. Bera, N. Chattopadhyay, Phys. Chem. Chem. Phys. 1 (1999) 3253.
[47] P. Purkayastha, Ph. D. Thesis, Jadavpur University (to be submitted).
[48] P. Purkayastha, S.C. Bera, N. Chattopadhyay, J. Mol. Liquids 88 (2000) 33.
[49] P. Purkayastha, N. Chattopadhyay, J. Mol. Struct., 570 (2001) 147.
[50] C.J.F. Böttcher, Theory of Electronic Polarization, Vol. I, Elsevier, Amsterdam, 1983.
[51] C.J. Cramer, D.G. Truhlar, in: P. Politzer, J.S. Murray (Eds.), Quantitative Treatment of Solute/Solvent Interaction, Vol. I, Elsevier, Amsterdam, 1994.
[52] N. Nandi, K. Bhattacharyya, B. Bagchi, Chem. Rev. 100 (2000) 2013.